Ampère and Hall nonlinearities in the magnetic dynamo in the Arnol'd–Beltrami–Childress (ABC) flow

B. Galanti[a)]
Department of Aerospace Engineering, Israel Institute of Technology, Technion City, 32000 Haifa, Israel

N. Kleeorin[b)]
Department of Mechanical Engineering, The Ben-Gurion University of the Negev, 84105 Beer-Sheva, Israel

I. Rogachevskii
Racah Institute of Physics, The Hebrew University of Jerusalem, 91904 Jerusalem, Israel

(Received 3 May 1995; accepted 26 July 1995)

The effect of different nonlinearities (Ampère force and Hall effect) on the saturation of a magnetic field generated by flows of conducting fluid is studied by means of numerical simulations. A three-fluid (i.e., ions, electrons, and neutral particles) model is considered. The velocity field of the neutral particles is a prescribed, deterministic, incompressible three-dimensional field in the form of the Arnol'd–Beltrami–Childress (ABC) flow. The dynamics of the charged components of fluid is determined by two-fluid magnetohydrodynamics when ion–neutral particle collisions are taken into account. Four typical regimes of the nonlinear evolution of the magnetic field, corresponding to different types of nonlinearities (Ampère force or Hall effect) and different types of collisions (ion–ion collisions or ion–neutral particle collisions) are found. The transitions between these regimes, the structure of the saturated magnetic field, and the evolution of the magnetic field in these regimes are studied. Scaling estimates of the level of the saturated magnetic field and conditions obtained for the different regimes of the magnetic field evolution are in agreement with the results of the numerical simulations. © *1995 American Institute of Physics.*

I. INTRODUCTION

Investigations of the nonlinear mechanisms of saturation of the growth of the magnetic field caused by flows of conducting fluid are important from the point of view of the theory of the generation of magnetic fields and various cosmic and laboratory applications.[1–6] A number of publications on the turbulent nonlinear dynamo[7–19] and the laminar nonlinear dynamo[20–22] have concentrated on the study of one-fluid magnetohydrodynamics (MHD). In the laminar dynamo the velocity field of the conducting fluid is deterministic, whereas in the turbulent dynamo it is random.

Recently, in the framework of two-fluid MHD, the nonlinear evolution of the magnetic field has been investigated for a deterministic[23] and turbulent[24,25] velocity field. The nonlinearity in these studies is due to the Hall effect. The influence of the magnetic field on the motion of the ions is negligibly small. Therefore this nonlinear dynamo model is kinematic in the sense that the evolution of the magnetic field is determined by a prescribed velocity field.

In the present paper we study dynamical effects. This means that together with the Hall effect we take into account the influence of the Ampère force on the motion of the ions. We consider a three-fluid (i.e., ions, electrons, and neutral particles) model. The motion of the neutral particles is chosen as a prescribed deterministic incompressible three-dimensional flow in the form of the ABC flow, since its properties are well studied.[26–37] The dynamics of the charged components of the fluid is determined by two-fluid MHD when taking into account ion–neutral particle collisions. This model represents weakly ionized plasma, where the effect of the charged component of the plasma on the motion of the neutral particles is negligibly small. Examples of such media include ionospheric plasma at low altitudes and laboratory plasma.[38–41] Four typical regimes of the nonlinear evolution of the magnetic field corresponding to different types of nonlinearities (Ampère force or Hall effect) and different types of collisions (ion–ion collisions or ion–neutral particle collisions) are found here. The transitions between these regimes are studied numerically. The structure of the saturated magnetic field and the evolution of the magnetic field in these cases are investigated.

II. THE GOVERNING EQUATIONS

We consider three-fluid MHD for electrons, ions, and neutral particles. The momentum equations for electrons and ions are given by[42,41]

$$m_i n_i \left(\frac{d\mathbf{v}_i}{d\tau}\right) = -\nabla p_i + z e n_i \mathbf{E} + \frac{z e n_i}{c}(\mathbf{v}_i \times \mathbf{b}) + \frac{m_e n}{\tau_{ei}} \times (\mathbf{v}_e - \mathbf{v}_i) + \frac{m_i n_i}{\tau_{in}}(\mathbf{u} - \mathbf{v}_i), \tag{1}$$

$$m_e n \left(\frac{d\mathbf{v}_e}{d\tau}\right) = -\nabla p_e - e n \mathbf{E} - \frac{e n}{c}(\mathbf{v}_e \times \mathbf{b}) - \frac{m_e n}{\tau_{ei}}(\mathbf{v}_e - \mathbf{v}_i) + \frac{m_e n}{\tau_{en}}(\mathbf{u} - \mathbf{v}_e), \tag{2}$$

$$\nabla \cdot \mathbf{u} = \nabla \cdot \mathbf{v}_i = \nabla \cdot \mathbf{v}_e = 0; \quad \nabla \cdot \mathbf{b} = 0, \tag{3}$$

[a)]Present address: Department of Chemical Physics, Weizmann Institute of Science, Rehovot 76100, Israel.
[b)]E-mail: nat@menix.bgu.ac.il
[c)]E-mail: gary@vms.huji.ac.il

where

$$\frac{d\mathbf{v}}{d\tau}=\frac{\partial\mathbf{v}}{\partial\tau}+(\mathbf{v}\cdot\nabla)\mathbf{v},$$

$\mathbf{v}_e$, $\mathbf{v}_i$, and $\mathbf{u}$ are the electron, ion, and neutral particle velocities, respectively, m_e and m_i are the electron and ion masses, p_e and p_i are the electron and ion pressures, τ_{in}, τ_{en}, and τ_{ei} are the ion–neutral, electron–neutral, and electron–ion collision times, respectively, ze is the ion charge, e is the electron charge, n is the electron number density, n_i is the ion number density, and c is the light speed. The relationship $zn_i=n$ is due to the electrical quasineutrality of plasma, $\mathbf{E}$ is the electric field, and $\mathbf{b}$ is the magnetic field.

We neglect the inertia of electrons $m_e n(d\mathbf{v}_e/dt)$ in Eq. (2) because $m_e \ll m_i$. Ohm's law follows from Eq. (2):

$$\mathbf{j}=\sigma\left(\mathbf{E}+\frac{1}{4\pi en}\mathbf{b}\times(\nabla\times\mathbf{b})+\frac{1}{c}\mathbf{v}_i\times\mathbf{b}+\frac{\nabla p_e}{en}\right), \tag{4}$$

where the electric current is $\mathbf{j}=en(\mathbf{v}_e-\mathbf{v}_i)$, $\nabla\times\mathbf{b}=(4\pi/c)\mathbf{j}$ and we consider for simplicity the case $\tau_{ei}\ll\tau_{en}$. The electrical conductivity is then $\sigma=e^2n\tau_{ei}/m_e$. The second term in Ohm's law describes the Hall effect.

When the electric field $\mathbf{E}$ is taken out of Eq. (4) and substituted into the Maxwell equation

$$\frac{\partial\mathbf{b}}{\partial\tau}=-c(\nabla\times\mathbf{E}) \tag{5}$$

we obtain the induction equation:

$$\frac{\partial\mathbf{b}}{\partial\tau}=\nabla\times\left(\mathbf{v}_i\times\mathbf{b}+\frac{c}{4\pi en}\mathbf{b}\times(\nabla\times\mathbf{b})-\eta\nabla\times\mathbf{b}\right), \tag{6}$$

where $\eta=c^2/4\pi\sigma$ is the magnetic diffusivity. The second term in Eq. (6) describes the Hall effect.

The sum of Eqs. (1)–(2) yields

$$m_i n_i\left(\frac{d\mathbf{v}_i}{d\tau}\right)=-\nabla p+\frac{1}{c}(\mathbf{j}\times\mathbf{b})+\frac{m_i n_i}{\tau_{in}}(\mathbf{u}-\mathbf{v}_i), \tag{7}$$

where $p=p_i+p_e$, and we take into account that $m_e\ll m_i$. The second term in Eq. (7) describes the influence of the magnetic field on the motion of plasma. It follows from Eqs. (4)–(7) that this term corresponds to a cubic nonlinearity $(\sim b^3\tau_i/4\pi m_i n_i l_b)$ in terms of the magnetic field in the induction equation. Here τ_i is the characteristic time of the ion component of the plasma and l_b is the characteristic scale of the magnetic field variations. In contrast, the nonlinearity in the induction equation caused by the Hall effect [the second term in Eq. (6)] is a quadratic nonlinearity in terms of the magnetic field.

Now let us compare these two kind of nonlinearities. First, we consider the case $\tau_{in}\gg\tau_i$. It follows from Eq. (7) that the variation of the ion velocity δv_i under the influence of the generated magnetic field is

$$\delta v_i\sim\frac{\tau_i}{m_i n_i c}|\mathbf{j}\times\mathbf{b}|.$$

The cubic nonlinearity is not as effective as the quadratic if

$$|\delta\mathbf{v}_i\times\mathbf{b}|\ll\left|\frac{c}{4\pi en}\mathbf{b}\times(\nabla\times\mathbf{b})\right|.$$

This leads to the following criterion:

$$\omega_{Hi}\tau_i\ll 1, \tag{8}$$

where $\omega_{Hi}=eb/(m_i c)$ is the ion gyrofrequency. When the ion characteristic time τ_i is much longer than τ_{in}, the Hall nonlinearity is dominated if

$$\omega_{Hi}\tau_{in}\ll 1. \tag{9}$$

In the intermediate case, when $\tau_i\sim\tau_{in}$, the criterion (8) coincides with (9).[23]

The case of the quadratic nonlinearity caused by the Hall effect $(\omega_{Hi}\tau_i\ll 1)$ was considered in Ref. 23. This corresponds to two-fluid MHD. On the other hand, the case of the cubic nonlinearity in the dynamo of ABC flow in one-fluid MHD was studied in Ref. 22. In the present paper we investigate the more general case where both nonlinearities (Ampère force and the Hall effect) may be of the same order of magnitude. We also study the effect of ion–neutral particle coupling on the evolution of the magnetic field. The following system of momentum and induction equations is solved numerically:

$$\frac{\partial\mathbf{V}_i}{\partial t}+(\mathbf{V}_i\cdot\nabla)\mathbf{V}_i=-\nabla P+(\nabla\times\mathbf{B})\times\mathbf{B}+T(\mathbf{U}-\mathbf{V}_i)+R_e^{-1}\Delta\mathbf{V}_i+\mathbf{f}_{\mathrm{ABC}}, \tag{10}$$

$$\frac{\partial\mathbf{B}}{\partial t}=\nabla\times[\mathbf{V}_i\times\mathbf{B}+\Lambda\mathbf{B}\times(\nabla\times\mathbf{B})]+R_m^{-1}\Delta\mathbf{B}, \tag{11}$$

$$\nabla\cdot\mathbf{V}_i=0,\quad \nabla\cdot\mathbf{B}=0. \tag{12}$$

Equations (10)–(11) are written in dimensionless variables: coordinates, velocity, and time are measured in the units $l_0=k_0^{-1}$, u_0, and τ_0, respectively; the magnetic field B is measured in units of $B_0=u_0(4\pi m_i n_i)^{1/2}$, the kinematic Reynolds number is $R_e=l_0^2/(\tau_0\nu)$, ν is the kinematic viscosity, the magnetic Reynolds number is $R_m=l_0^2/(\tau_0\eta)$, the body force is $\mathbf{f}_{\mathrm{ABC}}=-R_e^{-1}\Delta\mathbf{U}_{\mathrm{ABC}}$, where $\mathbf{U}_{\mathrm{ABC}}$ is the ABC flow, and P is the pressure measured in the units $m_i n_i u_0^2$. Here we take into account a small but finite kinematic viscosity of the ions ν. The dimensionless parameters of the system are given by

$$\Lambda=(\Omega_{Bi}\tau_0)^{-1},\quad T=\tau_0/\tau_{in},$$

where $\Omega_{Bi}=eB_0/m_i c$ and T, Λ are positive control parameters. Different values of the parameters determine the various regimes of solutions. The criterion (9) can be rewritten as

$$B/\Lambda T\ll 1. \tag{13}$$

This condition corresponds to the predominance of the Hall nonlinearity. In this case the main balance in the induction equation is

$$|\mathbf{V}_i\times\mathbf{B}|\sim\Lambda|\mathbf{B}\times(\nabla\times\mathbf{B})|. \tag{14}$$

On the other hand, the influence of the Ampère force on the motion of fluid can be neglected, i.e.,

$$|\mathbf{B}\times(\nabla\times\mathbf{B})| \ll T|\mathbf{U}-\mathbf{V}_i|. \tag{15}$$

It follows from Eq. (14) that the level of the magnetic field in saturation is given by

$$B \sim 1/\Lambda. \tag{16}$$

Here we take into account that $|\mathbf{U}| \sim |\mathbf{V}_i| \sim O(1)$. Substituting (16) in (13) yields the condition for when the Hall nonlinearity dominates

$$\Lambda^2 T \gg 1. \tag{17}$$

Note that in this regime $T \gg R_e^{-1}$. This case corresponds to a two-fluid (electron–ion) model and was studied in detail in Ref. 23. This regime is called the $\mathscr{H}$ regime.

Now we consider an opposite case, when the influence of the magnetic field on the motion of ions is strong and the Hall effect is not substantial. This means that the main balance in the momentum equation is

$$|\mathbf{B}\times(\nabla\times\mathbf{B})| \sim T|\mathbf{U}-\mathbf{V}_i|, \tag{18}$$

whereas in the induction equation the nonlinear in $\mathbf{B}$ term is small:

$$|\mathbf{V}_i\times\mathbf{B}| \gg \Lambda|\mathbf{B}\times(\nabla\times\mathbf{B})|. \tag{19}$$

Condition (18) yields the saturation level of the magnetic field $B \sim T^{1/2}$. This case corresponds to a two-fluid (ion–neutral particles) model. This regime is called the $\mathscr{C}$ regime.

The $\mathscr{C}$ regime can be interpreted in terms of "ambipolar diffusion" (see, e.g., Refs. 43–45). The ambipolar diffusion is taken into account in the term $T(\mathbf{U}-\mathbf{V}_i)$ in the momentum equation (10). In order to get the coefficient of the ambipolar diffusion we take the velocity $\mathbf{V}_i$ from Eq. (18) and substitute it in the induction equation (11). It yields after simple manipulation the total diffusion coefficient η_0 in the nondimensional form

$$\eta_0 = \frac{B^2}{T} + \frac{1}{R_m}, \tag{20}$$

where the second term determines the magnetic diffusivity whereas the first term is the nonlinear coefficient of the ambipolar diffusion. Equation (19) allows us to obtain more rigorous estimation of the level of magnetic field in saturation for the $\mathscr{C}$ regime. If $\eta_0 = 1/R_m^{\rm cr}$, where $R_m^{\rm cr}$ is the critical magnetic Reynolds number for excitation of the magnetic field, then the level of magnetic field in saturation for the $\mathscr{C}$ regime is given by

$$B \sim T^{1/2}\left(\frac{1}{R_m^{\rm cr}} - \frac{1}{R_m}\right)^{1/2}, \quad R_m > R_m^{\rm cr}. \tag{21}$$

Criterion (19) is reduced to

$$\Lambda T^{1/2}\left(\frac{1}{R_m^{\rm cr}} - \frac{1}{R_m}\right)^{1/2} \ll 1, \tag{22}$$

where $T \gg R_e^{-1}$ and we take into account Eq. (21).

When time of ion–neutral particle collisions is much longer than the characteristic time τ_0 (i.e., $T \ll 1$; R_e^{-1}), the main balance in the momentum equation is

$$|\mathbf{B}\times(\nabla\times\mathbf{B})| \sim R_e^{-1}|\Delta\mathbf{V}_i| \tag{23}$$

and the condition (19) is still valid. It follows from (23) that the level of the magnetic field in saturation in this case is given by

$$B \sim R_e^{-1}, \tag{24}$$

and criterion (19) is reduced to

$$R_e^{-1/2}\Lambda \ll 1. \tag{25}$$

This case corresponds to the one-fluid MHD model and was studied in Ref. 22. This regime is called the $\mathscr{B}$ regime.

III. NUMERICAL SIMULATIONS

The nonlinear equations (10)–(11) have been solved numerically in a 2π-periodic domain. The time-marching scheme is a second-order Adams–Bashforth scheme in which diffusion is treated exactly. The nonlinear terms are calculated using a Fourier (pseudo)-spectral method in space. Since the calculation of the nonlinear terms is the major part of the whole computation, an attempt to minimize the number of fast Fourier transforms (FFT) has been made. For a three-dimensional Navier–Stokes equation eight FFT's are required.[46] The number of FFT's increases to 14 when solving the induction equation and three additional FFT's are needed when including the pure Hall nonlinearity. This is in comparison with the computation of the pure nonlinear Hall effect that requires only nine FFT's (see Ref. 23).

The velocity field of neutral particles $\mathbf{U}$ is given as an ABC flow:

$$\begin{aligned}\mathbf{U} = \mathbf{U}_{\rm ABC} = [&A\sin(k_0 z) + C\cos(k_0 y),\\ &B\sin(k_0 x) + A\cos(k_0 z),\\ &C\sin(k_0 y) + B\cos(k_0 x)],\end{aligned} \tag{26}$$

with $A = B = C = 1$ and the wave number $k_0 = 1$.

The computations have been tested against various previous known simulations. In particular, the solution was compared for $T = 0$ and $\Lambda = 0$ to that obtained in Ref. 22 and for $\mathbf{V}_i = \mathbf{U} = \mathbf{U}_{\rm ABC}$ and $\Lambda = 1$ to that in Ref. 23.

Our focus in this computation is on the behavior of the full nonlinear system (10)–(11) and the study the different contributions of the various nonlinearities. There are four control parameters as they appear in Eqs. (10)–(11), namely, T, Λ, R_e, and R_m. A complete study of the full parameter space is very difficult, and therefore we choose to reduce it to the most important two-dimensional parameter space: (T, Λ). The kinematic and magnetic Reynolds numbers are kept constant $R_e = R_m = 12$. For this value of kinematic Reynolds number, the velocity field is found stable hydrodynamically (see Refs. 31 and 33). Moreover, this value of magnetic Reynolds number belongs to the first dynamo window of the kinematic problem, and ensures a maximal growth rate of the magnetic field in this window (see Ref. 30). Since the magnetic Reynolds establishes the smallest scale of the magnetic field, the number of modes in the present simulation is as much as necessary to resolve all existing scales. In particular, the number of modes for $R_m = R_e = 12$ is 16^3. This relatively low resolution simulation enables an extensive and fine study of the parameter space and the obtaining of the precise location of the various re-

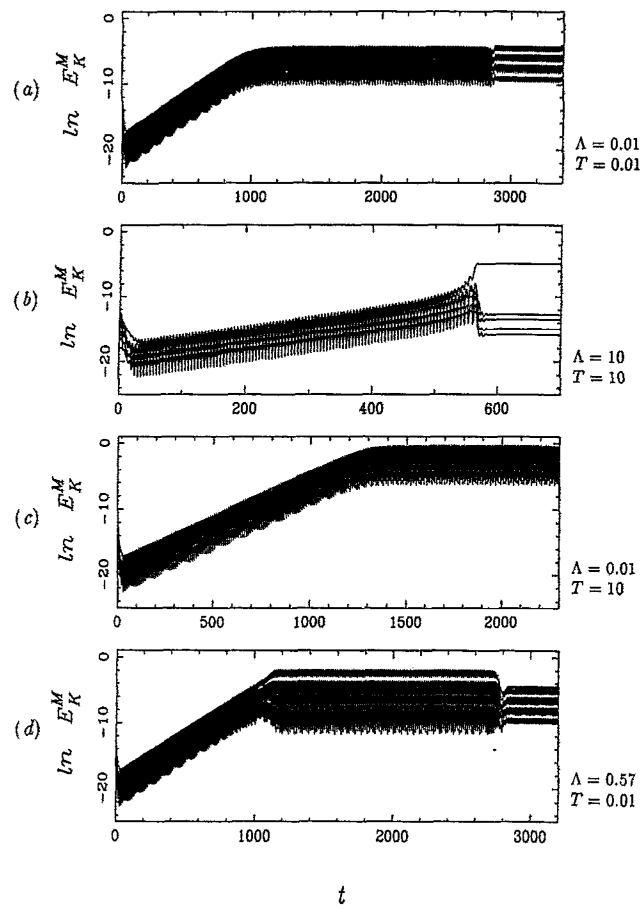

FIG. 1. Time evolution of the magnetic energy modes E_K^M for different Λ and T that corresponds to four characteristic types of magnetic field evolution: (a) $\mathcal{B}$ regime; (b) $\mathcal{H}$ regime; (c) $\mathcal{C}$ regime; (d) $\mathcal{T}$ regime.

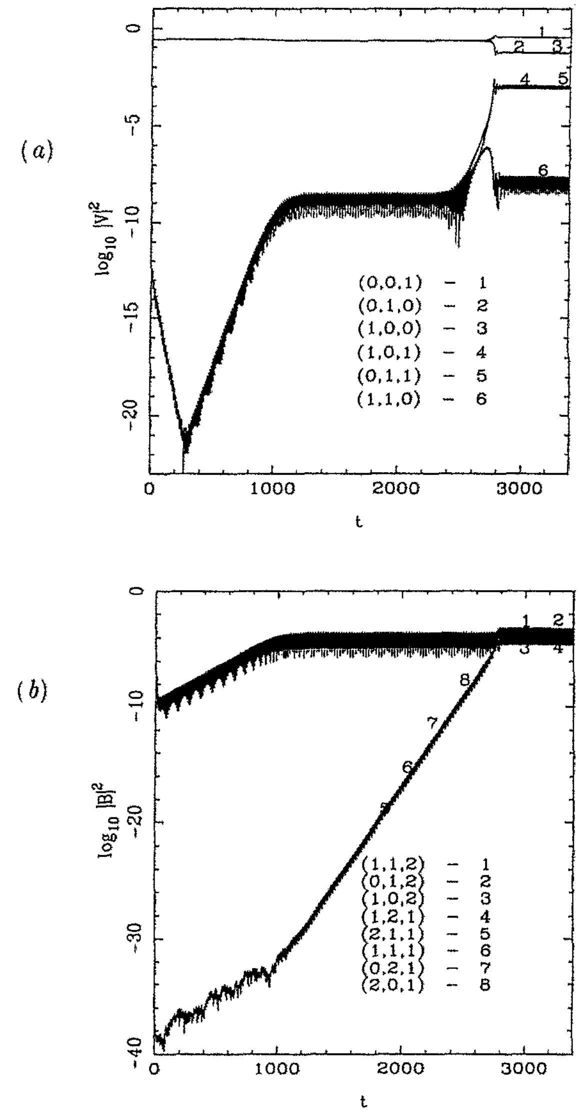

FIG. 2. Time evolution of the magnetic energy of $\mathcal{B}$ regime for the main mode $K=1$ and mode $K>1$ before the symmetry breaking ($\Lambda=0.01$, $T=0.01$).

gimes in the phase space. For all simulations, a given weak seed magnetic field is taken as an initial condition.

Figure 1 shows the time evolution of the magnetic energy modes $E_K^M = \frac{1}{2}\Sigma_{|\mathbf{k}|\in C_K}|\mathbf{B}_{|\mathbf{k}|}|^2$ in spherical shells $C_K=\{K-\frac{1}{2}\leq|\mathbf{k}|<K+\frac{1}{2}\}$. Here $\mathbf{k}$ is the wave-number vector and K is the number of the spherical shell. The six most energetic shells are shown. Four characteristic examples of the time evolution of the magnetic energy are presented. Figure 1(a) corresponds to a regime where the Hall effect is not substantial ($\Lambda=0.01\ll 1$) and the characteristic time of ion–neutral particle collisions is very long in comparison with τ_0 (i.e., $T=0.01\ll 1$, R_e^{-1}). In this case the criterion $R_e^{-1/2}\Lambda\ll 1$ is valid. The main nonlinearity that results in the saturation of growth of the magnetic field at $t\approx 1000$ is the Ampère force. The level of the magnetic field is approximately determined by Eq. (23) and it is of the order of $B\sim R_e^{-1/2}$. This case may be described by the one-fluid MHD model and is identified as the $\mathcal{B}$ regime.

Note that at $t=t_{sb}\approx 2850$ there is an abrupt change in the magnetic energy. This transition is typical to this regime. The ABC flow for the case $A=B=C$ has 24 symmetries.[26] The magnetic field which has some of the symmetries of the ABC flow in the primary saturation,[30] loses them by symmetry breaking at $t=t_{sb}$ and stabilizes in a secondary saturation at $t>t_{sb}$. A similar transition was found in Ref. 22. Starting from a given random initial condition the magnetic field grows exponentially and then stabilizes in a form similar to that of the $\mathcal{C}$ regime (see below). After a relatively long time, marginally unstable weak modes of the magnetic and velocity fields with $K>1$ become important and interact with stable modes of the magnetic and velocity fields (see Fig. 2). The result of this nonlinear coupling is a rapid transition and stabilization into a new configuration, i.e., a symmetry breaking.

In Fig. 3(a) the contour surfaces of the magnetic field $|\mathbf{B}|$ at two instants are shown: at $t=2000$ (before the symmetry breaking) and $t=3200$ (after the symmetry breaking). It is seen that before the symmetry breaking the magnetic field is concentrated within cigar-like forms close to the four α-type stagnation points of the ABC flow. For $t>t_{sb}$ the cigar-like forms of the magnetic field completely collapse.

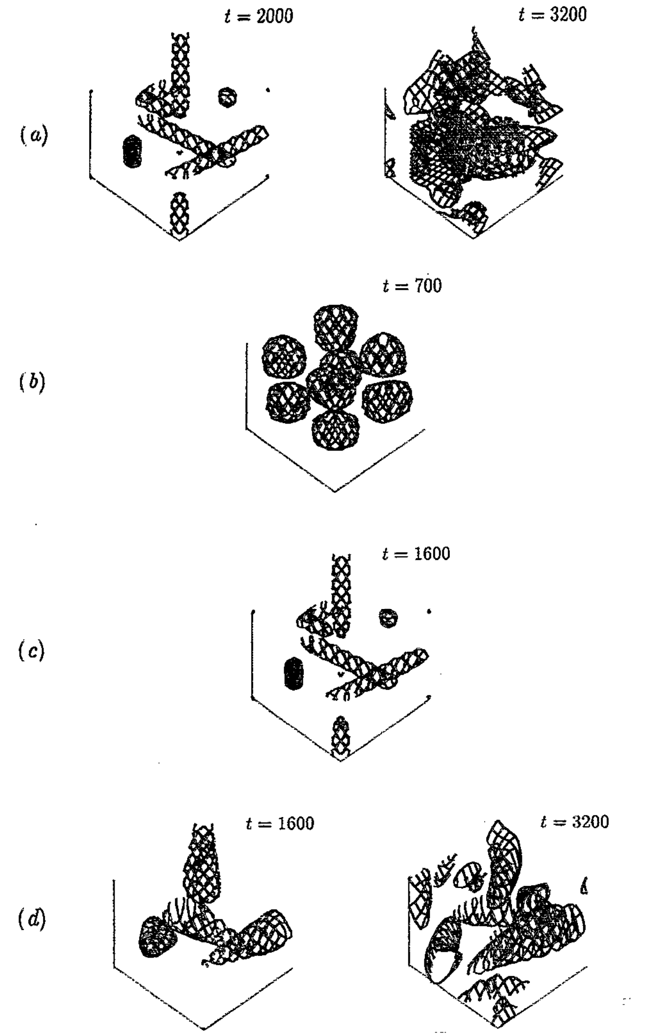

FIG. 3. The contour surfaces of the magnetic field $|\mathbf{B}|$ for four characteristic types of magnetic field evolution: (a) $\mathscr{B}$ regime; (b) $\mathscr{H}$ regime; (c) $\mathscr{C}$ regime; (d) $\mathscr{T}$ regime.

Figure 1(b) displays an opposite limiting case where the Hall effect is dominant ($\Lambda=10$), and the influence of the magnetic field on the motion of the ions is negligibly small. The level of the magnetic field in saturation is determined by Eq. (14). It is given by $B \sim \Lambda^{-1}$ and found to be in good agreement with the numerical results. The oscillations which characterize the linear regime die away, leading to a steady-state solution without oscillations. The distribution of the energy in the different energy modes shows that the energy in the first energy shell E_1 has a much more significant magnitude than that of the remaining E_K^M for $K>1$ (see Ref. 23). The structure of the magnetic field in this case [see Fig. 3(b)] is entirely different from that of the pure Ampère nonlinearity case [Fig. 3(a)]. This regime is the $\mathscr{H}$ regime.

In the case of the $\mathscr{H}$ regime symmetry breaking does not occur. The solutions typical of the $\mathscr{H}$ regime have in general different symmetry groups compared to the symmetries of the ABC flow.[23] The marginally unstable modes with $K>1$ observed in the $\mathscr{B}$ regime are not generated during the nonlinear evolution in the $\mathscr{H}$ regime and the velocity field is not changed in this regime.

Now we consider the case when the effect of the Ampère nonlinearity is much stronger than that of the Hall nonlinearity, and the ion–neutral particle collisions predominate over the ion–ion collisions (i.e., $T \gg R_e^{-1}$). The evolution of the magnetic field in this case is shown in Fig. 1(c) for $T=10$ and $\Lambda=0.01$. The level of the magnetic field in saturation in this case is determined by Eq. (21). The symmetry breaking does not appear here and the magnetic field keeps the cigar-like form [see Fig. 3(c)]. This regime is the $\mathscr{C}$ regime.

While the fact that the predominant nonlinearity in both the $\mathscr{B}$ and $\mathscr{C}$ regimes shown in Figs. 1(a) and 1(c) is the Ampère force, the main difference between these two cases is due to the mechanism of dissipation. In the regime shown in Fig. 1(c) the friction force $\mathbf{F}_f$ is independent of the inhomogeneity of the ion velocity and is determined by the ion–neutral particle collisions [i.e., when T is sufficiently large, and the friction force $\mathbf{F}_f = T(\mathbf{U}-\mathbf{V}_i)$]. On the other hand, the friction force in the case of symmetry breaking [Fig. 1(a)] is determined by ion–ion collisions and depends on the inhomogeneity of the ion velocity ($\mathbf{F}_f = R_e^{-1}\Delta \mathbf{V}_i$). Therefore, the difference in dissipations here determines the different mechanisms of reconstruction of the ion flows under the influence of the magnetic field. As follows from the numerical simulations, the change in the ion velocity in the vicinity of the region of generation of the magnetic field (the stagnation points) is not accompanied by a strong reconstruction of flows in the case of the $\mathscr{C}$ regime [Fig. 1(c)], whereas in the case of the $\mathscr{B}$ regime [Fig. 1(a)] reconstruction of the ion flow is substantial (up to the destruction of the stagnation points in the moment of symmetry breaking).

The $\mathscr{C}$ regime can be interpreted in terms of the ambipolar diffusion (see Sec. II). It was found by Refs. 45, 47, and 48 that the nonlinear nature of the ambipolar diffusion for large magnetic Reynolds number leads to the formation of both sharp structures in the magnetic field near magnetic nulls and extended force-free regions. The probability density function (PDF) for the ratio quantity

$$q = \frac{|\mathbf{B} \times (\nabla \times \mathbf{B})|}{|\mathbf{B}||(\nabla \times \mathbf{B})|}$$

was calculated for all regimes in order to find regions with force-free magnetic fields. The probability rises with q. The maximum of the PDF is always found where q tends to one. This indicates that we do not have any force-free magnetic fields. Note that there is a difference between the problems considered in our paper and those studied in Refs. 45, 47, and 48:

(a) We use a specific three-dimensional laminar velocity field in the form of an ABC flow with $\operatorname{div} \mathbf{U}=0$, whereas in Refs. 45, 47, and 48 the flows are two dimensional and $\operatorname{div} \mathbf{V}_D \neq 0$, where $\mathbf{V}_D = \mathbf{V}_i - \mathbf{U}$, $\mathbf{U}$ is the velocity of neutral particles, and $\mathbf{V}_i$ is the ion velocity.
(b) The most crucial parameter that determines the basic difference between our simulations and that considered in Refs. 45, 47, and 48 is the magnetic Reynolds number R_m. We use a low $R_m = 12$.

This difference is the reason why in the $\mathscr{C}$ regime there is no formation of sharp structures in the magnetic field near

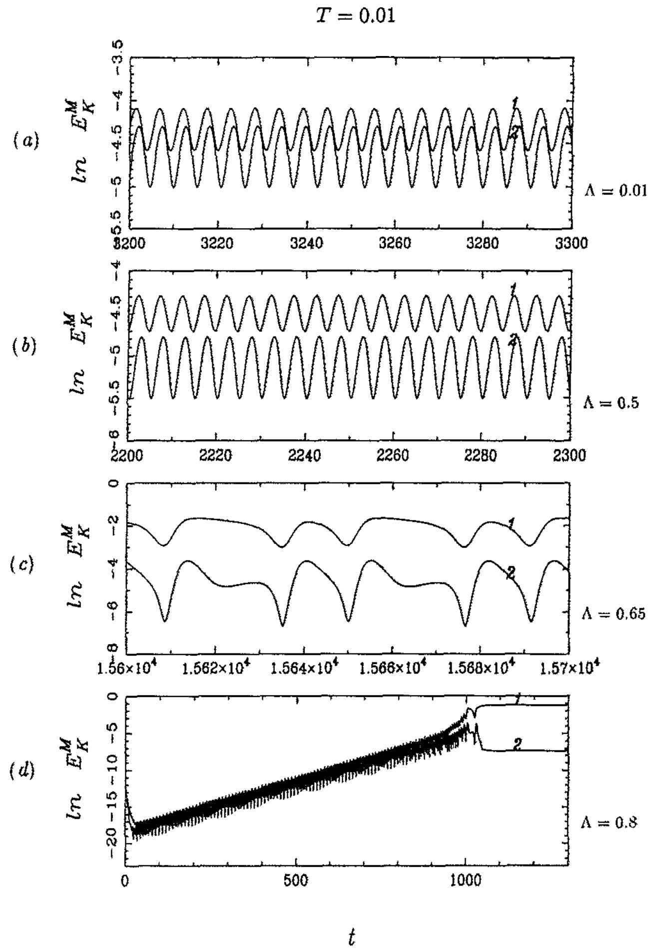

FIG. 4. Transition from the case of pure Ampère nonlinearity ($\Lambda=0.01$) to the case of pure Hall nonlinearity ($\Lambda\rightarrow1$) for $T=0.01$.

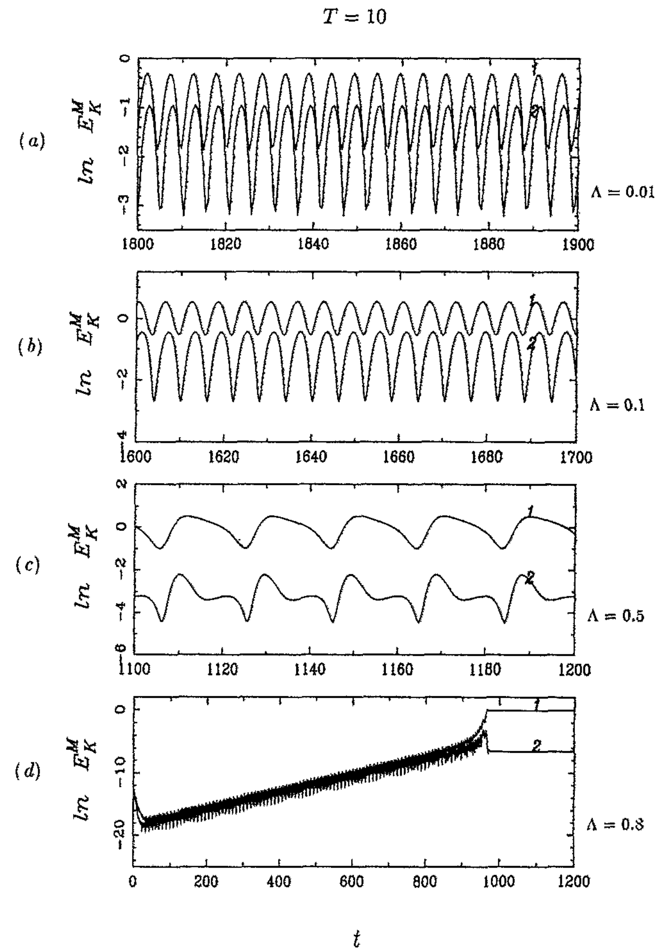

FIG. 5. Transition from the case of pure Ampère nonlinearity ($\Lambda=0.01$) to the case of pure Hall nonlinearity ($\Lambda\rightarrow1$) for $T=10$.

magnetic nulls and no formation of extended force-free regions. Near magnetic nulls in our case there is no generation of the magnetic field, because the generation of magnetic field in ABC flows occurs near the stagnation points of the velocity field (if they exist). There are no force-free structures in $\mathscr{B}$, $\mathscr{C}$, and $\mathscr{T}$ regimes because the presence of a nonzero Ampère force is a necessary condition for the existence of these regimes.

A rise in the parameter Λ results in an increase in the influence of the Hall effect on the evolution of the magnetic field. This is seen in Fig. 1(d) for the time interval $1000<t<2800$. This regime is the $\mathscr{T}$ regime. The energy in the first shell E_1 has a much more significant magnitude than that of the remaining E_K^M for $K>1$. The same property was found for the pure Hall effect regime [compare with Fig. 1(b)]. The structure of the magnetic field in this time interval can be considered as an intermediate stage between the case shown in the left picture of Fig. 3(a) and the blob-like structure that is typical for the pure Hall nonlinearity regime [see Fig. 3(b)]. At $t=2800$ symmetry breaking appears. The Hall effect in this case results in the structure of the magnetic field not being completely destroyed. Indeed, the traces of the cone-like forms are kept after the symmetry breaking [see Fig. 3(d) at $t=3200$].

Transition from the case of the pure Ampère nonlinearity ($\Lambda=0.01$) to the case of the pure Hall nonlinearity ($\Lambda\sim1$) is presented in Fig. 4 for $T=0.01$ and in Fig. 5 for $T=10$. The quasiharmonic oscillations of the function $\ln E_K^M$ that are typical for the pure Ampère nonlinearity [see Figs. 4(a) and 5(a)] are transformed to essentially unharmonic oscillations when Λ grows. The period of these oscillations increases with the increase in Λ. The oscillations fade away in the case of the pure Hall nonlinearity. Quasiharmonic oscillations of the magnetic energy for the pure Ampère nonlinearity can be related to Alfvén waves propagating along the magnetic field lines. In the case of the pure Hall nonlinearity (when there is no influence of the magnetic field on the motion of plasma), the oscillations of the magnetic field disappear, and thus the transformation of energy from the magnetic field into the flow of plasma vanishes and Alfvén waves cannot exist.

Regions of parameters in the $\log\Lambda-\log T$ diagram corresponding to different regimes are shown in Fig. 6. The boundaries between different regimes can be determined in the following way. The boundary between $\mathscr{H}$ regime (the case of pure Hall nonlinearity) and the $\mathscr{C}$ regime can be found by means of the comparison of conditions (17) and (22). The result is given by

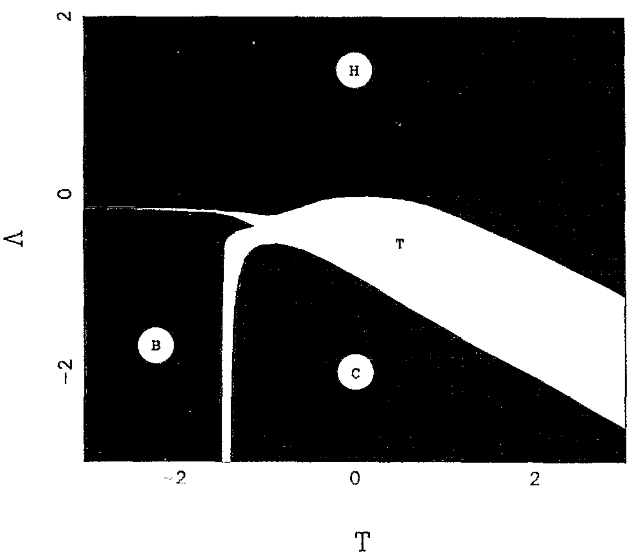

FIG. 6. Diagram log Λ−log T of regions of parameters that correspond to different regimes of magnetic field evolution.

$$\Lambda \sim T^{-1/2}\left(\frac{1}{R_m^{\rm cr}}-\frac{1}{R_m}\right)^{-1/2}. \tag{27}$$

The boundary between the $\mathscr{H}$ regime and $\mathscr{B}$ regime can be obtained from (25) and (17):

$$\Lambda \sim R_e^{1/2}. \tag{28}$$

Finally, the boundary between $\mathscr{B}$ regime and $\mathscr{C}$ regime can be found by means of the condition $T|\mathbf{U}-\mathbf{V}_i| \sim R_e^{-1}|\Delta \mathbf{V}_i|$. Therefore this boundary is determined by

$$T \sim R_e^{-1}. \tag{29}$$

Criteria (27)–(29) as well as estimations of the level of the saturated magnetic field (16), (21), and (24) are in satisfactory agreement with the numerical simulations.

IV. CONCLUSIONS

The influence of nonlinearities (the Ampère force and the Hall effect) on the saturation of the magnetic field generated by flows of conducting fluid is investigated numerically. A three-fluid (i.e., ions, electrons, and neutral particles) model is considered. The velocity field of neutral particles is a prescribed deterministic incompressible three-dimensional field in the form of the ABC flow. The dynamics of charged components of fluid is determined by two-fluid MHD when taking into account ion–neutral particle collisions. Four different regimes of the nonlinear evolution of the magnetic field corresponding to different types of nonlinearities (Ampère force or Hall effect) and different types of collisions (ion–ion collisions or ion–neutral particle collisions) are found. The transitions between these regimes, structure of the saturated magnetic field, and evolution of the magnetic field in these regimes are studied. Analytical scalings for the level of the saturated magnetic field and derived conditions for the different regimes of the magnetic field evolution are in satisfactory agreement with results of the numerical simulation.

In this paper the Ampère and the Hall nonlinearities were investigated for constant magnetic (R_m) and kinematic (R_e) Reynolds numbers. Many interesting questions arise regarding this problem. The main one is how the different regimes mentioned above (or new ones) take form in the limit of large magnetic and kinematic Reynolds numbers. It is well known that the velocity field undergoes several bifurcations and for sufficiently large R_e it becomes fully turbulent. Another possible approach is to investigate the problem for different coefficients of the ABC flow or for other deterministic flows (which are kinematic dynamo too). It is known[30,31] that the case where $A=B=C$ is highly symmetrical compared to any other combination of ABC flow coefficients, thus we expect that some of the regimes will be absent or degenerate.

ACKNOWLEDGMENTS

We thank A. Gilbert and the referee for very useful suggestions.

The work was supported in part by the Israel Ministry of Science.

[1] H. K. Moffatt, *Magnetic Field Generation in Electrically Conducting Fluids* (Cambridge University Press, New York, 1978).
[2] E. Parker, *Cosmical Magnetic Fields* (Oxford University Press, New York, 1979), and references therein.
[3] F. Krause and K. H. Rädler, *Mean-Field Magnetohydrodynamics and Dynamo Theory* (Pergamon, Oxford, 1980), and references therein.
[4] Ya. B. Zeldovich, A. A. Ruzmaikin, and D. D. Sokoloff, *Magnetic Fields in Astrophysics* (Gordon and Breach, New York, 1983).
[5] A. Ruzmaikin, A. M. Shukurov, and D. D. Sokoloff, *Magnetic Fields of Galaxies* (Kluwer Academic, Dordrecht, 1988).
[6] Ya. B. Zeldovich, A. A. Ruzmaikin, and D. D. Sokoloff, *The Almighty Chance* (World Scientific, Singapore, 1990).
[7] M. Stix, Astron. Astrophys. **20**, 9 (1972).
[8] G. Rüdiger, Astron. Nachr. **295**, 229 (1974).
[9] S. A. Jepps, J. Fluid Mech. **67**, 625 (1975).
[10] P. N. Roberts and A. M. Soward, Astron. Nachr. **296**, 49 (1975).
[11] T. S. Ivanova and A. A. Ruzmaikin, Sov. Astrophys. J. **21**, 479 (1977).
[12] M. Meneguzzi, U. Frisch, and A. Pouquet, Phys. Rev. Lett. **41**, 1060 (1981).
[13] J. Leorat, U. Frisch, and A. Pouquet, J. Fluid Mech. **104**, 419 (1981).
[14] A. Brandenburg, F. Krause, R. Meinel, D. Moss, and I. Tuominen, Astron. Astrophys. **213**, 411 (1989).
[15] N. Kleeorin, I. Rogachevskii, and A. Ruzmaikin, Sov. Phys. JETP **70**, 878 (1990).
[16] R. M. Kulsrud and S. W. Anderson, Astrophys. J. **396**, 606 (1991).
[17] N. Kleeorin and I. Rogachevskii, Phys. Rev. E **50**, 2716 (1994).
[18] N. Kleeorin, I. Rogachevskii, and A. Ruzmaikin, Sol. Phys. **155**, 223 (1994).
[19] N. Kleeorin, I. Rogachevskii, and A. Ruzmaikin, Astron. Astrophys. **297**, 159 (1995).
[20] P. H. Roberts, in *Geomagnetism*, edited by J. A. Jacobs (Academic, London, 1987), Vol. 2, p. 251.
[21] K. K. Zhang and F. H. Busse, Geophys. Astrophys. Fluid Dyn. **44**, 33 (1988); **49**, 97 (1989).
[22] B. Galanti, P. L. Sulem, and A. Pouquet, Geophys. Astrophys. Fluid Dyn. **66**, 183 (1992).
[23] B. Galanti, N. Kleeorin, and I. Rogachevskii, Phys. Plasmas **1**, 3843 (1994).
[24] N. Kleeorin, I. Rogachevskii, and A. Eviatar, J. Geophys. Res. A **99**, 6475 (1994).
[25] N. Kleeorin and I. Rogachevskii, Phys. Rev. E **50**, 493 (1994).
[26] V. I. Arnol'd, C. R. Acad. Sci. Paris **261**, 17 (1965).
[27] M. Hénon, C. R. Acad. Sci. Paris **262**, 312 (1966).
[28] S. Childress, J. Math. Phys. **11**, 3063 (1970).

[29] V. I. Arnol'd, Ya. B. Zeldovich, A. A. Ruzmaikin, and D. D. Sokoloff, Sov. Phys. JETP **54**, 1083 (1981).
[30] D. J. Galloway and U. Frisch, Geophys. Astrophys. Fluid Dyn. **36**, 53 (1986).
[31] D. J. Galloway and U. Frisch, J. Fluid Mech. **180**, 557 (1987).
[32] T. Dombre, U. Frisch, J. M. Green, M. Hénon, A. Mehr, and A. M. Soward, J. Fluid Mech. **167**, 353 (1986).
[33] O. Podvigina and A. Pouquet, Physica D **75**, 471 (1994).
[34] G. M. Zaslavskii, R. Z. Sagdeev, and A. A. Chernikov, Sov. Phys. JETP **67**, 270 (1988).
[35] J. M. Finn and E. Ott, Phys. Fluids **31**, 2992 (1988); Phys. Fluids B **2**, 916 (1990).
[36] A. D. Gilbert and S. Childress, Phys. Rev. Lett. **65**, 2133 (1990).
[37] Y. T. Lau and J. M. Finn, Phys. Fluids B **2**, 916 (1993).
[38] S. I. Akasofu and S. Chapman, *Solar–Terrestrial Physics* (Clarendon, Oxford, 1972).
[39] H. Alfvén, *Cosmic Plasma* (Reidel, Dordrecht, 1981).
[40] *The Handbook of Plasma Physics*, edited by A. Galeev and R. Sudan (North-Holland, Amsterdam, 1983).
[41] F. F. Chen, *Introduction to Plasma Physics and Controlled Fusion* (Plenum, New York, 1984).
[42] S. I. Braginskii, in *Reviews of Plasma Physics*, edited by M. A. Leontovich (Consultants Bureau, New York, 1965), Vol. 1, p. 205.
[43] L. Mestel and L. Spitzer, Mon. Not. R. Astron. Soc. **116**, 503 (1956).
[44] R. M. Kulsrud and W. P. Pearce, Astrophys. J. **156**, 445 (1969).
[45] A. Brandenburg and E. G. Zweibel, Astrophys. J. **427**, L91 (1994).
[46] C. Basdevant, J. Comput. Phys. **50**, 209 (1983).
[47] A. Brandenburg and E. G. Zweibel, "Effects of pressure and resistivity on the antipolar diffusion singularity: Too little, too late," to appear in Astrophys. J. (1995).
[48] M. M. Mac Low, M. L. Norman, A. Konigl, and M. Wardle, Astrophys. J. **442**, 726 (1995).